BIOCHEMISTRY
including biophysical chemistry & molecular biology

Article

pubs.acs.org/biochemistry

Nitric Oxide Regulation of Cyclic di-GMP Synthesis and Hydrolysis in *Shewanella woodyi*

Niu Liu,[†] Yueming Xu,[†] Sajjad Hossain,[§] Nick Huang,[†] Dan Coursolle,[∥] Jeffrey A. Gralnick,[∥] and Elizabeth M. Boon*[,†,§,‡]

[†]Department of Chemistry, Stony Brook University, Stony Brook, New York 11794-3400, United States
[‡]Institute of Chemical Biology and Drug Discovery, Stony Brook University, Stony Brook, New York 11794-3400, United States
[§]Molecular and Cellular Biology Graduate Program, Stony Brook University, Stony Brook, New York 11794-3400, United States
[∥]Department of Microbiology, BioTechnology Institute, University of Minnesota, St. Paul, Minnesota 55108-6106, United States

Supporting Information

ABSTRACT: Although several reports have documented nitric oxide (NO) regulation of biofilm formation, the molecular basis of this phenomenon is unknown. In many bacteria, an H-NOX (heme-nitric oxide/oxygen-binding) gene is found near a diguanylate cyclase (DGC) gene. H-NOX domains are conserved hemoproteins that are known NO sensors. It is widely recognized that cyclic di-GMP (c-di-GMP) is a ubiquitous bacterial signaling molecule that regulates the transition between motility and biofilm. Therefore, NO may influence biofilm formation through H-NOX regulation of DGC, thus providing a molecular-level explanation for NO regulation of biofilm formation. This work demonstrates that, indeed, NO-bound H-NOX negatively affects biofilm formation by directly regulating c-di-GMP turnover in *Shewanella woodyi* strain MS32. Exposure of wild-type *S. woodyi* to a nanomolar level of NO resulted in the formation of thinner biofilms, and less intracellular c-di-GMP, than in the absence of NO. Also, a mutant strain in the gene encoding *Sw*H-NOX showed a decreased level of biofilm formation (and a decreased amount of intracellular c-di-GMP) with no change observed upon NO addition. Furthermore, using purified proteins, it was demonstrated that *Sw*H-NOX and *Sw*DGC are binding partners. *Sw*DGC is a dual-functioning DGC; it has diguanylate cyclase and phosphodiesterase activities. These data indicate that NO-bound *Sw*H-NOX enhances c-di-GMP degradation, but not synthesis, by *Sw*DGC. These results support the biofilm growth data and indicate that *S. woodyi* senses nanomolar NO with an H-NOX domain and that *Sw*H-NOX regulates *Sw*DGC activity, resulting in a reduction in c-di-GMP concentration and a decreased level of biofilm growth in the presence of NO. These data provide a detailed molecular mechanism for NO regulation of c-di-GMP signaling and biofilm formation.

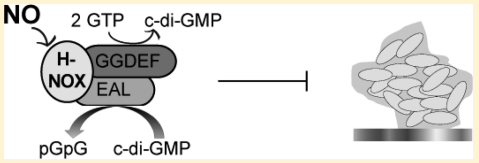

Most bacteria can switch between sessile and planktonic growth to adapt to varying environmental conditions. Biofilms, sessile, surface-attached bacterial communities, are widespread, persistent, and highly resistant to antibiotics.[1] Effective new strategies for controlling biofilms are needed, but the biochemical pathways underlying their regulation must first be elucidated.

Nitric oxide, a well-known signaling molecule in mammals,[2] has been shown to regulate bacterial biofilms at physiological concentrations. For example, in *Nitrosomonas europaea*, NO levels above 30 ppb result in biofilm formation and below 5 ppb in biofilm dispersal.[3] NO also plays an important signaling role in biofilm dispersal in the cystic fibrosis-associated pathogen *Pseudomonas aeruginosa*.[4] The dispersal of *P. aeruginosa* biofilms was observed upon treatment with the NO donor sodium nitroprusside at 25 nM, a sublethal concentration. Taking advantage of the observation that NO can disperse biofilms, multiple labs developed several methods to treat biofilms using NO-releasing materials.[5−7] Despite these observations, the NO signaling pathway that regulates biofilm formation is not known.

Biofilm formation is a complex process with fundamental regulatory mechanisms still widely debated.[8] Nonetheless, it is clear that bis-(3′−5′)-cyclic dimeric guanosine monophosphate (cyclic di-GMP or c-di-GMP) is a secondary messenger widely used by bacteria to regulate biofilm formation.[9−11] As the intracellular concentration of c-di-GMP increases, bacteria enter biofilm or persistence growth modes.[12] The intracellular concentration of c-di-GMP is controlled through two enzymatic activities. Diguanylate cyclases synthesize c-di-GMP from two molecules of GTP, and phosphodiesterases hydrolyze c-di-GMP to pGpG. Diguanylate cyclase activity is predicted by a conserved GGDEF amino acid motif;[13] similarly, EAL[12] or HD-GYP[14] amino acid motifs are conserved in phosphodiesterases for the degradation of c-di-GMP. Thus, in bacteria, GGDEF and EAL or HD-GYP domains inversely regulate c-di-GMP levels.[15]

Invariably, there are input sensory domains associated with GGDEF and EAL/HD-GYP domains, suggesting that c-di-

Received: November 27, 2011
Revised: February 22, 2012
Published: February 23, 2012

dx.doi.org/10.1021/bi201753f | *Biochemistry* 2012, 51, 2087−2099

Table 1. Strains, Plasmids, and Primers Used in This Work

	relevant characteristics	ref
bacterial strains		
S. woodyi		
*Sw*MS32 (WT)	*S. woodyi* MS32, ATCC 51908	36
Δ*hnox*	*Sw*MS32 Δ*Swoo_2751*	this work
Δ*hnox*/p*hnox*	*Sw*MS32 Δ*hnox* p*hnox*, Km^r	this work
E. coli		
WM3064	mating strain	25
BL21(DE3) pLysS	expression strain	
plasmids		
pSMV3	deletion vector, Km^r, *sacB*	25
pBBR1MCS-2	broad range cloning vector, Km^r	27
pΔ*hnox*	pSMV3 with 1 kb upstream and downstream of *hnox*	this work
p*hnox*	pBBR1MCS-2 with *hnox* and 32 bp upstream of *hnox*	this work
	Primers	
gene deletion primers		
*Sw*2751-up-fw	NNNGGATCCCACATAGTTTGGACACCTAAG[a]	
*Sw*2751-up-rev	NNNGAATTCAACATTAGCCCCTGTTTTAA[a]	
*Sw*2751-down-fw	NNNGAATTCTTATGAGTGCACTTGAGGACA[a]	
*Sw*2751-down-rev	NNNNNNNNNGCGGCCGCCACAATAGAGAACTCATCTC[a]	
confirmation primers		
hnox-up-fw	GGATCTGCTCCGCTTGC	
hnox-down-rev	GGTTACTTTGTTGACACAGTGG	
complementation primers		
hnox-comp 1	CAACGAATTCGAGTACTTATTAAAAC	
hnox-comp 2	CAAACTCGAGACGTCGTGTAATATTA	

[a]N represents a random nucleobase that is designed to protect restriction sites.

GMP concentrations are controlled by signal transduction from a variety of environmental stimuli.[16] Stimuli known to regulate c-di-GMP formation and hydrolysis include blue light,[17] intercellular molecules,[18] and oxygen.[19] Interestingly, the Kjelleberg group has shown that NO mediates phosphodiesterase activity to enhance biofilm dispersal in *P. aeruginosa*;[20] the NO sensor and NO-sensitive phosphodiesterase have not been identified, however.

H-NOX (heme-nitric oxide/oxygen-binding) domains make up a family of hemoprotein sensors that include the heme domain of soluble guanylate cyclase (sGC), the well-studied mammalian NO sensor.[21] Like sGC, bacterial H-NOX proteins bind NO sensitively and selectively.[22−25] Bioinformatics studies have revealed that several common effectors may be associated with H-NOX, including methyl-accepting chemotaxis proteins, histidine kinases, and diguanylate cyclases.[26] Biochemical studies have indicated that NO-bound H-NOX is capable of regulating the enzymatic activity of associated effectors in several species.[27−29] For example, an H-NOX in *Legionella pneumophila* has been found to inhibit biofilm formation, likely through regulation of an associated diguanylate cyclase.[27] Direct evidence of H-NOX and diguanylate cyclase interaction and the mechanism of NO regulation of cyclase activity has not been demonstrated, however.

We have previously shown that *Swoo_2750* (*Sw*DGC) from *Shewanella woodyi* strain MS32 (*Sw*MS32; cross-listed as strain ATCC 51908) has both c-di-GMP synthesis and hydrolysis activities, as predicted from the presence of a GGDEF domain and an EAL domain in its primary structure.[30] Here we demonstrate that NO regulates biofilm formation in *S. woodyi* through changes in c-di-GMP concentration and that *Sw*H-NOX (*Swoo_2751*) and *Sw*DGC are responsible for this NO biofilm phenotype. Furthermore, these results indicate that *Sw*H-NOX and *Sw*DGC directly interact and that NO-bound H-NOX regulates the enzymatic activity of *Sw*DGC. The data presented here reveal for the first time a molecular mechanism detailing NO regulation of c-di-GMP metabolism and biofilm formation.

EXPERIMENTAL PROCEDURES

Materials and General Methods. All reagents were purchased in their highest available purity and used as received.

Bacterial Strains and Growth Conditions. Strains used in this study are listed in Table 1. *Escherichia coli* strains DH5α, BL21(DE3)pLysS, Tuner(DE3)pLysS, and Rossetta2(DE3) were used throughout this study for plasmid amplification and protein purification. *E. coli* were typically grown in Luria broth (LB, 20 g/L, EMD chemicals) at 37 °C with agitation at 250 rpm. *E. coli* strain WM3064 was used as a donor for conjugation and was grown in LB complemented with 2,3-diaminopropionic acid (DAP, 0.36 mM, Sigma Aldrich) at 37 °C with agitation at 250 rpm (VWR International). *Sw*MS32 was grown in Marine Media Broth (MM, 28 g/L, BD Difco) at 25 °C with agitation at 250 rpm. *Sw* transconjugants were grown on LB (10 g/L)/MM (14 g/L)/Bacto Agar (BA, 10 g/L, BD Difco) plates at 25 °C.

Construction of In-Frame Gene Disruption Mutant Strains. Polymerase chain reaction (PCR) was used to amplify regions of genomic DNA flanking the H-NOX gene (*Swoo_2751*) from *S. woodyi* strain MS32 genomic DNA (ATCC strain 51908) using Phusion polymerase (New England Biolabs). The upstream genomic DNA was amplified with forward and reverse primers (*Sw*2751-up-fw and *Sw*2751-up-rev, respectively) containing *Not*I and *Eco*RI restriction sites, respectively. The downstream genomic DNA was amplified with forward and reverse primers [*Sw*2751-down-fw and

*Sw*2751-down-rev, respectively (Table 1)] containing *Eco*RI and *Bam*HI restriction sites, respectively. The up- and downstream fragments were fused by ligation at the common *Eco*RI restriction site. This fused product was cloned into pSMV3[31] using the *Not*I and *Bam*HI restriction sites and sequenced (Stony Brook DNA sequencing facility). The resulting vector [pΔ*hnox* (Table 1)] was transformed into plasmid donor strain *E. coli* WM3064 and grown on LB/DAP/BA plates with kanamycin added to a concentration of 10 μg/mL. WM3064 transformed with the deletion vector was mated with *Sw*MS32 in a 1:3 ratio on LB/MM/DAP plates for 2 days at 25 °C. The *S. woodyi* transconjugants containing the deletion vector were selected on LB/MM/BA plates supplemented with 60 μg/mL kanamycin and verified by colony PCR [*hnox*-up-fw and *hnox*-down-rev (Table 1)]. The selected colonies were then plated on LB/MM/BA plates containing 5% sucrose at 25 °C to select for double-recombination events. Plates were then replica printed onto LB/MM/BA plates with and without added kanamycin (60 μg/mL) at 25 °C; kanamycin-sensitive colonies were screened by colony PCR for gene deletion using primers *hnox*-up-fw and *hnox*-down-rev (Table 1).

Construction of Gene Disruption Mutant Complementation Plasmids. PCR was used to amplify *Swoo_2751* from *S. woodyi* genomic DNA (ATCC) using Pfu Turbo polymerase (Agilent). Upstream and downstream primers contained *Bam*HI and *Eco*RI restriction sites, respectively, as well as 26 bp of upstream target gene sequence, so that all ribosome binding sites would be identical [*hnox*-comp 1 and *hnox*-comp 2 (Table 1)]. The amplified PCR products were cloned into the broad host range plasmid pBBR1MCS-2[32] and sequenced (Stony Brook DNA sequencing facility). The resulting p*hnox* plasmid (Table 1) was introduced into the gene-disrupted strains via conjugation as previously described.[31]

Biofilm Imaging by Confocal Microscopy. Microscopy images were recorded on a Zeiss LSM 510 Metanlo Two-Photon Laser Scanning Confocal Microscope System. Fifteen milliliters of a 1:1000 dilution of an overnight culture of *S. woodyi* in MM was added to a sterile 50 mL conical centrifuge tube containing a glass microscope slide. Biofilms were grown under steady-state conditions at 25 °C with slow agitation at 50 rpm for 24 h. Following the growth period, the slide was thoroughly rinsed with distilled water and the adhered biofilm cells were stained with the LIVE/DEAD *Bac*Light kit (Invitrogen), according to the manufacturer's protocol, for 15 min. The biofilm formed at the air−liquid interface was then imaged and analyzed. The air−liquid interface was ∼3 mm wide (in the *X* dimension, along the longest side of the microscope slide), as determined from crystal violet staining of identically obtained biofilms on microscope slides. The biofilm thickness (*X*−*Z* dimension, i.e., the height of the biofilm measured from the surface of the microscope slide to the top of the biofilm) was measured at three different locations in each experiment and averaged to determine the mean biofilm thickness. The locations were chosen randomly, but generally one spot near the middle of the slide and one from each edge of the slide (in the *Y* dimension) were chosen. Multiple locations were measured because bacterial biofilms are often not of uniform thickness. These measurements may not account for all the variation in biofilm thickness, but they provide an estimate of biofilm thickness for comparison between wild-type and Δ*hnox* mutant *S. woodyi* strains. Biofilm mass was quantified using crystal violet staining (see below). Confocal images for each of three independently grown biofilms of each strain (wild-type and Δ*hnox* mutant *S. woodyi*) were separately obtained and analyzed. The mean thickness from each trial was determined from measurements at multiple locations. The mean thickness from three independent trials ± one standard deviation is reported.

Crystal Violet (CV) Staining for Biofilm Quantification. Steady-state biofilm formation, at the air−liquid interface, in a shaking culture was examined in 96-well polyvinyl chloride (PVC) plates as previously described,[33] with a few modifications. A 100 μL subculture (1:100 dilution of an overnight culture of *S. woodyi*) in MM was incubated at 25 °C for 24 h with slow agitation (50 rpm). The planktonic cells and media were then removed, and the remaining biofilm was rigorously washed with water followed by staining with 200 μL of 0.1% CV in water for 15 min. Next the CV solution was removed, and the wells were rinsed three times with distilled water and allowed to thoroughly dry. Then 100 μL of DMSO was added to each well to solubilize the CV adsorbed by the biofilm cells. The DMSO/CV solution was removed from the PVC plate and added to a polystyrene 96-well plate, and the OD_{570} was measured with a Perkin-Elmer Victor X5 multilabel reader. The data are reported as the CV absorbance at 570 nm divided by the optical density of the planktonic and biofilm cells at 600 nm. For biofilms grown in the presence of NO, the 100-fold diluted overnight culture was diluted into MM supplemented with 200 μM diethylenetriamine NONOate (DETA/NO, Cayman Chemicals; for DETA/NO, $t_{1/2}$ = 20 and 56 h at 37 and 22−25 °C, respectively) that had been decaying for 20 h at 37 °C (approximately one half-life; it was cooled to 25 °C before inoculation). NONOates are NO-donating compounds that are stable as solids but spontaneously release NO in a pH-dependent manner in solution. Using a Nitric Oxide Analyzer 280i (Sievers), it was determined that this resulted in a solution NO concentration of <100 nM (slowly decreased from ∼80 to ∼60 nM) during the length of NO exposure. From there, the protocol was identical. Each biofilm condition was run a minimum of 10 times in one experiment, and the entire experiment was performed a minimum of three times. The mean ± one standard deviation is reported.

Quantification of c-di-GMP. Intracellular c-di-GMP concentrations were quantified as described previously,[34] with slight modifications. Briefly, a single *S. woodyi* wild-type or mutant colony from a MM/BA plate was grown to an optical density of 1.5 at 600 nm at 25 °C with agitation at 250 rpm in MM. Cultures were then diluted 1:1000 and grown at 25 °C with agitation at 250 rpm for 24 h. Formaldehyde (final concentration of 0.18%) was then added to prevent c-di-GMP degradation. One milliliter of this culture was pelleted by centrifugation at 6000 rpm for 5 min. The pellet was then resuspended in 400 μL of ice-cold extraction buffer (40% methanol, 40% acetonitrile, 0.1% formic acid, and 19.9% Milli-Q water) and vortexed for 30 s followed by incubation on ice for 15 min. The resultant lysates were centrifuged at 14000 rpm for 5 min, and the pellets were discarded. The supernatant was then dried by rotary evaporation, and the remaining pellet was resuspended in 50 μL of Milli-Q water. c-di-GMP was separated and quantified for each sample by high-performance liquid chromatography (HPLC) (Shimadzu LC-2010A HT) using a Shimadzu Shimpack XR-ODS c-8 column. Separations were conducted in a 0.1 M TEAA (triethylammonium acetate) solution (pH 6.0) at a rate of 0.1 mL/min with 10% methanol. The c-di-GMP concentration was determined by comparison to a standard curve generated from known concentrations of c-di-

GMP (Biolog Life Science Institute) run on the HPLC system under identical conditions. The HPLC peak assigned to c-di-GMP was confirmed by MALDI mass spectrometry (a peak in the mass spectrum at m/z 691 was observed; the expected mass for c-di-GMP is 690 g/mol). To introduce NO, 50 μM diethylamine NONOate (DEA/NO, Cayman Chemicals; for DEA/NO, $t_{1/2}$ = 2 and 16 min at 37 and 22−25 °C, respectively) was added 20 min before the cells were harvested. The DEA/NO had been predecayed at 25 °C before addition to the *S. woodyi* cultures. A Nitric Oxide Analyzer 280i (Sievers) was used to determine that the solution NO concentration was <100 nM (decayed from ∼80 to ∼50 nM) during the length of NO exposure in these experiments. The result was normalized by cell mass. Each data set was independently obtained a minimum of three times. The mean c-di-GMP concentration, relative to the wild-type strain, ± one standard deviation is reported.

Protein Expression and Purification. *Sw*DGC and mutants were expressed and purified as previously described.[30] PCR was used to amplify *Swoo_2750* from *S. woodyi* genomic DNA (ATCC) using Expand polymerase (Roche). Upstream and downstream primers contained *Nde*I and *Xho*I restriction sites, respectively. The amplified PCR product was cloned into pET-20b (Novagen) and sequenced. Cell culture procedures for *Sw*H-NOX were conducted as previously described for other H-NOX proteins.[22] Purification of the *Sw*H-NOX protein took advantage of the C-terminal His_6 tag; *Sw*H-NOX was purified by metal affinity chromatography (Ni-NTA) followed by gel filtration (Superdex 200 HiLoad 26/60).

Electronic Spectroscopy. All electronic spectra were recorded on a Cary 100 spectrophotometer equipped with a constant-temperature bath. Preparation of the various ligation complexes of H-NOX was conducted as previously published.[22]

NO Dissociation Rate. NO dissociation rates were measured as previously described.[22] Briefly, Fe^{2+}−NO complexes of protein (final heme concentration of 5 μM) diluted in anaerobic 50 mM HEPES, 50 mM NaCl buffer (pH 7.5) were rapidly mixed with an anaerobic solution of 30 mM (final concentration) dithionite ($Na_2S_2O_4$) saturated with carbon monoxide (CO) in the same buffer.[22,35,36] It has been previously established that CO binding is not rate-limiting in these experiments;[35] this was confirmed in experiments using only 30 mM $Na_2S_2O_4$ without CO as a trap. Data were acquired by scanning periodically on a Cary 100 spectrophotometer equipped with a constant-temperature bath set to 20 °C. The dissociation of NO from the heme was monitored as the formation of the Fe^{2+}−CO complex at 423 nm. Difference spectra were calculated by subtracting the first scan from each subsequent scan. The NO dissociation rate was determined from the increase in absorbance at 423 nm versus time and fit with a single or two parallel exponentials of the form $f(x) = A(1 - e^{-kx})$. Each experiment was performed a minimum of six times, and the resulting rates were averaged. The dissociation rates measured are independent of CO and dithionite concentration (3, 30, and 300 mM dithionite were tested).

Pull-Down Assay. Glutathione *S*-transferase (GST) fusions of *Sw*DGC, *Sw*GGAAF, and *Sw*AAL were created by subcloning *Sw*DGC and mutants from pET28b(+) into a pGEX4t-2 (GE Life Science) vector by PCR amplification using Pfu Turbo polymerase. Upstream and downstream primers contained *Bam*HI and *Xho*I restriction sites, respectively. GST constructs were purified from Rosetta2(DE3) cells (induced with 250 μM IPTG overnight at 16 °C). Glutathione Sepharose beads with protein bound were washed in 50 mM Tris, 300 mM NaCl, 1 mM PMSF, 2 mM DTT, and 0.5% Triton X-100. Following washing, 10 μM His_6-tagged *Sw*H-NOX was added to the beads in a final volume of 1 mL in the same buffer and incubated overnight at 4 °C with gentle rocking. Beads were then washed three times with the same buffer and then boiled in 50 μL of SDS sample buffer. Ten microliters of this reaction mixture was loaded onto a 12.5% Tris glycine gel for Western blot analysis. Polyclonal anti-His antibody (Abcam) was used in 5% milk to detect the presence of His_6-tagged *Sw*H-NOX.

Steady-State Kinetics Analysis. Steady-state kinetic parameters for diguanylate cyclase activity were determined using *Sw*AAL. *Sw*AAL (50 nM) was incubated with various concentrations of GTP (0.5−50 μM) at 25 °C in buffer containing 75 mM Tris-HCl (pH 7.5), 250 mM NaCl, 25 mM KCl, and 10 mM $MgCl_2$. Initial velocities were determined by following the production of pyrophosphate (PP_i) using the PhosphoWorks kit (AAT bioquest) on a Perkin-Elmer Victor X5 multilabel reader. In this assay, PP_i (a c-di-GMP coproduct of diguanylate cyclase activity) is detected by a turn-on fluorescent PP_i sensor. To obtain the actual product concentration (used for calculation of the initial velocity and other kinetic parameters), the raw values of the fluorescence versus time data were normalized to a standard curve generated by plotting the fluorescence of known concentrations of commercial pyrophosphate detected using the PhosphoWorks assay.

Steady-state kinetic parameters for phosphodiesterase activity were determined using *Sw*GGAAF. *Sw*GGAAF (50 nM) was incubated with various concentrations of c-di-GMP (0.5−25 μM) at 25 °C in buffer containing 50 mM Tris and 1 mM $MgCl_2$ (pH 7.5). Initial velocities were determined by following the production of phosphate using a modified Invitrogen EnzChek kit on a Cary 100 spectrophotometer equipped with a constant-temperature bath set to 25 °C. One unit of calf intestinal phosphatase (CIP from New England Biolabs, 10 units/mL) was added to the kit contents to convert the product pGpG to phosphate (for detection by EnzChek) and GpG. To obtain the actual product concentration (used for calculation of the initial velocity and other kinetic parameters), we normalized the raw values of the absorbance versus time data to a standard curve generated by plotting the absorbance of known concentrations of commercial pGpG (Biolog) detected using the modified EnzChek assay.

In both assays, the initial velocity (V_i) was determined by plotting the corresponding product concentration versus time and fitting the data with the linear regression formula ([product] = $V_i t + C$), where C is basal absorbance and t is time. V_{max} and K_M were determined by plotting V_i versus substrate concentration and fitting with the Michaelis−Menten equation [$V_i = (V_{max}[substrate])/([substrate] + K_M)$]. k_{cat} was calculated from V_{max} ($k_{cat} = V_{max}/[enzyme]$). Origin 7.0 was used for all fittings. In reaction mixtures containing *Sw*H-NOX, preincubation of *Sw*H-NOX (varying concentrations, 1−20 μM) with *Sw*AAL or *Sw*GGAAF was conducted for 20 min at 25 °C before the addition of substrate to initiate the reaction. All of the coupling enzymes used in the EnzChek assay as well as including CIP were determined not to be rate-limiting [doubling the concentration of each coupling enzyme did not affect the initial velocity measured (see Table S3 of the Supporting Information)].

RESULTS

Despite intense research efforts, regulation of biofilm development is not well-understood.[1] However, it has become apparent that the signaling molecule NO plays a role in biofilm development.[3,4,20] To provide molecular details concerning how NO affects biofilm growth, in this report we investigate our hypothesis that NO influences biofilm formation through H-NOX regulation of c-di-GMP metabolism.

Correlation of Biofilm Thickness on *Sw*H-NOX. To determine if H-NOX plays a role in biofilm growth in *S. woodyi*, biofilms of wild-type and Δ*hnox* mutant *S. woodyi* strains were grown on microscope slides. Deletion of the *Sw*H-NOX gene does not lead to any delay in cell growth (Figure S1 of the Supporting Information). Biofilms formed at the air−liquid interface were stained with SYTO9 (green; stains live cells) and propidium iodide (red; stains dead cells only) and imaged by confocal microscopy.[37] In this experiment, the thickness and density of biofilm formation, as well as cell viability, can be visualized. As illustrated in Figures 1 and 2, wild-type *S. woodyi* forms robust biofilms under aerobic conditions. We call *S. woodyi* biofilms robust because we consistently obtain thick, well-adhered films; the cells are not easily scraped off the surface, and one can see a band of cells at the liquid−air interface. As shown in Figure 1, in comparison to the wild type, deletion of *Sw*H-NOX results in a visible decrease in the density and thickness of the biofilm formed (average biofilm coverage, ∼100% for *Sw*MS32 and ∼50% for Δ*hnox*; average biofilm thicknesses, 6.9 ± 0.4 μm for *Sw*MS32 and 5.0 ± 0.9 μm for Δ*hnox*). In all cases, the biofilm cells were healthy; live and dead staining indicated few dead cells. Therefore, we conclude that *Sw*H-NOX affects the appearance of biofilms in *S. woodyi*. These findings led us to further investigate, and quantify, the role of *Sw*H-NOX and NO in biofilm formation.

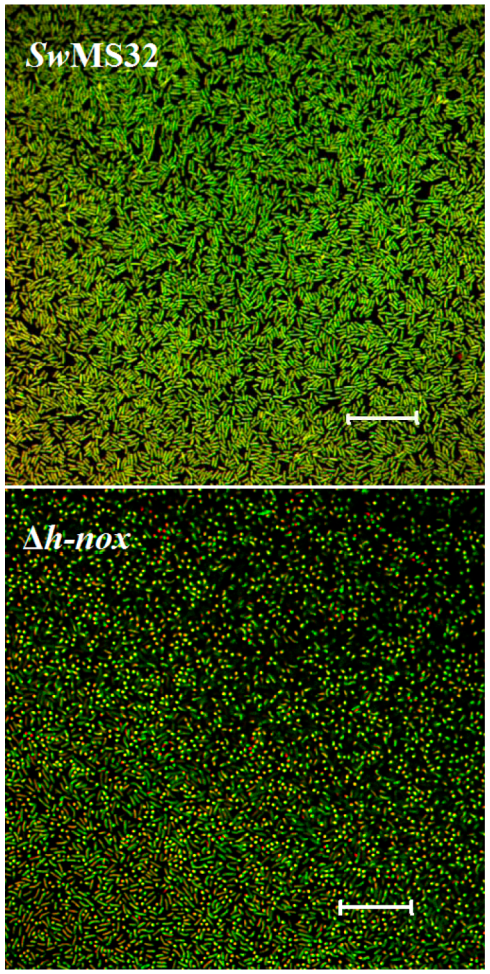

Figure 1. *Sw*H-NOX regulates biofilm formation. Biofilms of wild-type and Δ*hnox* mutant *S. woodyi* stained with SYTO9 (green; stains all cells) and propidium iodide (red; stains dead cells) and imaged by confocal laser scanning microscopy. The top is an *X*−*Y* view of a *Sw*MS32 biofilm; the bottom is an *X*−*Y* view of a Δ*hnox* biofilm. The bar is 20 μm.

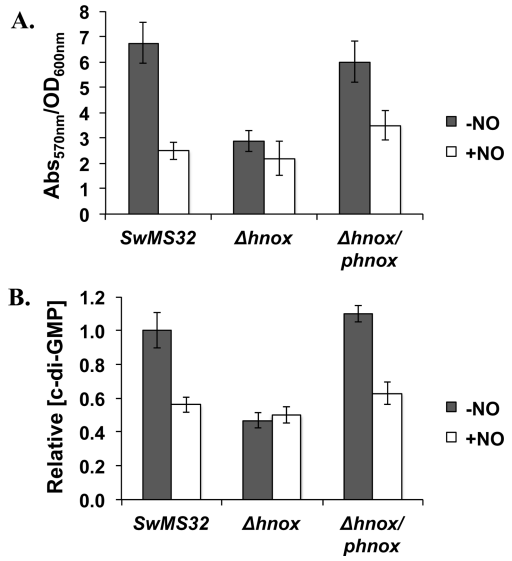

Figure 2. *Sw*H-NOX mediates an NO-dependent reduction in intracellular c-di-GMP concentration and biofilm formation. (A) Biofilms of wild-type and Δ*hnox* mutant *S. woodyi* formed at the liquid−air interface of PVC plates after growth for 24 h, in the presence and absence of NO (gradual decrease from ∼80 to ∼60 nM during the 24 h growth period), quantified by CV staining. Each biofilm condition was run a minimum of 12 times in one experiment, and the entire experiment was performed a minimum of three times. The mean ± one standard deviation is reported. (B) Intracellular c-di-GMP concentrations of wild-type and Δ*hnox* mutant *S. woodyi* in the presence and absence of NO (decrease from ∼80 to ∼50 nM during exposure). The c-di-GMP concentration relative to the concentration of c-di-GMP in *Sw*MS32 in the absence of NO (∼1400 pmol/mg of cells) is reported. Each data set was independently obtained a minimum of three times. The mean c-di-GMP concentration, relative to that of the wild type, ± one standard deviation is reported. Taken together, these data indicate that *Sw*H-NOX and *Sw*DGC regulate biofilm formation in response to NO through c-di-GMP concentration changes.

Effect of NO/H-NOX on c-di-GMP Concentration and Biofilm Thickness in *S. woodyi*. Having established that *Sw*H-NOX affects biofilm growth in *S. woodyi*, we sought to quantify the effect of NO and *Sw*H-NOX on biofilm formation. Biofilms of wild-type and mutant *S. woodyi* were grown in the presence and absence of NO. Biofilm growth at the air−liquid interface was analyzed by crystal violet staining of biofilms grown in a 96-well plate.[27]

All of the biofilm experiments reported here were open to air, and diethylenetriamine NONOate (DETA/NO) was used as an NO donor.[38] NONOates are stable as solids but spontaneously release NO in a pH-dependent manner in solution.[39] The nonlethal concentration range of NONOate

dx.doi.org/10.1021/bi201753f | *Biochemistry* 2012, 51, 2087−2099

was determined using planktonic growth curves measured with exposure to varying concentrations of NONOate (Figure S1 of the Supporting Information). We established that NONOates are nontoxic (no decrease in OD relative to no NONOate) up to ~1 mM with our strains under the conditions tested. Further, the concentration of NO in solution throughout the entire length of the biofilm experiment was measured using a Nitric Oxide Analyzer 280i (Sievers). By allowing the NONOate (for DETA/NO, $t_{1/2}$ = 20 and 56 h at 37 and 22−25 °C, respectively) to decay for approximately one half-life before inoculation, the NO concentration throughout the experiment stayed relatively constant for more than 24 h. Under the experimental conditions used here, 200 μM DETA/NO resulted in a relatively steady concentration of <100 nM NO (slowly decayed from ~80 to ~60 nM) during the full course of biofilm growth. This is consistent with solution (cell medium) NO concentrations previously reported using DETA/NO.[40,41]

Figure 2A illustrates the results of biofilm growth after 24 h analyzed by crystal violet staining. The amount of biofilm observed in the absence (filled bars) and presence (empty bars) of NO is compared for wild-type and Δ*hnox* strains. The key observations are as follows. First, the wild-type strain exhibits a marked decrease in the level of biofilm growth in the presence of a nanomolar concentration of NO. Second, the *Sw*H-NOX gene is required for this NO biofilm phenotype, as evidenced by a decreased level of biofilm in the Δ*hnox* strain both with and without NO. Finally, the decreased biofilm phenotype activity in the Δ*hnox* construct is correlated with the absence of *Sw*H-NOX, as complementation of the deletion strain with the *hnox* gene on a plasmid restores wild-type activity.

To determine if the decrease in the extent of biofilm growth observed in Figures 1 and 2A was, as we hypothesized, correlated with a decrease in cellular c-di-GMP levels, we quantified the amount of c-di-GMP present in *S. woodyi* cell lysates in the presence and absence of NO. In these experiments, *S. woodyi* strains were exposed to <100 nM NO from DEA/NO for 20 min before c-di-GMP extraction. This short NO exposure was designed to maximize the changes in c-di-GMP concentration resulting from changes in enzyme activity and minimize the possibility of changes in c-di-GMP concentration caused by changes in gene expression.

As illustrated in Figure 2B, the c-di-GMP quantification results are consistent with the biofilm growth experiments. A decrease in the concentration of c-di-GMP in the wild-type strain (wild type [c-di-GMP] is ~1400 pmol c-di-GMP/mg of cells) upon exposure to NO, and a similar decrease in the Δ*hnox* strain in both the presence and absence of NO was observed. For the Δ*hnox* mutant, plasmid complementation with the deleted gene restores wild-type activity. These data imply that the changes in biofilm growth observed in the presence of NO and/or the absence of *Sw*H-NOX (Figure 2A) are the direct result of changes in the concentration of cellular c-di-GMP.

A reasonable NO sensing and signaling mechanism that would result in these data is one in which NO is sensed by *Sw*H-NOX, and that NO-bound *Sw*H-NOX decreases the c-di-GMP output of *Sw*DGC. This reduction in c-di-GMP production ultimately results in a decrease in the extent of biofilm formation.

Steady-State Kinetics of the Diguanylate Cyclase and Phosphodiesterase Activities of *Sw*DGC. To begin to explore the hypothesis that NO/H-NOX affects c-di-GMP concentrations and biofilm formation in *S. woodyi* through direct regulation of *Sw*DGC, we first determined the steady-state kinetics of each enzymatic activity of *Sw*DGC. In our previous study, we found *Sw*DGC to have both diguanylate cyclase and phosphodiesterase activities.[30] We have confirmed that the activity of one domain (e.g., phosphodiesterase activity in the EAL domain) is not affected by a point mutation in the other domain [e.g., the GGDEF to GGAAF mutation in the cyclase domain does not affect phosphodiesterase activity (see Tables S1 and S2 of the Supporting Information)]. Thus, to simplify product detection and quantification, here, we measured the kinetics of each activity separately using point mutants that inactivate one active site or the other. As we have shown previously,[30] *Sw*AAL has only diguanylate cyclase activity (condensation and cyclization of two molecules of GTP to c-di-GMP) due to mutation of a key residue in the active site of the phosphodiesterase domain. *Sw*GGAAF, on the other hand, has only phosphodiesterase activity (hydrolysis of c-di-GMP to pGpG).

To measure diguanylate cyclase activity, the production of pyrophosphate (PP_i), which along with c-di-GMP is a product of diguanylate cyclase activity, by *Sw*AAL was monitored. A range of GTP concentrations were tested to obtain k_{cat} and K_M values for *Sw*AAL. As illustrated in Figure 3A and Table 2 (see additional controls in Table S1 of the Supporting Information), in the absence of *Sw*H-NOX, *Sw*AAL has a k_{cat} of 0.105 ± 0.005 s^{-1}, a K_M of 7.74 ± 0.90 μM, and a k_{cat}/K_M of 0.014 s^{-1} μM^{-1}. In comparison to those of other diguanylate cyclases, these kinetics indicate that *Sw*AAL has moderate diguanylate cyclase activity. The cyclase activity of *Sw*AAL is similar to that of PleD (k_{cat} = 0.102 ± 0.023 s^{-1}; K_M = 5.8 ± 1.2 μM; k_{cat}/K_M = 0.018 s^{-1} μM^{-1}) and lower than that of WspR (k_{cat} = 4.50 ± 0.12 s^{-1}; K_M = 5.97 ± 0.80 μM; k_{cat}/K_M = 0.75 s^{-1} μM^{-1}).[42,43]

To determine the phosphodiesterase activity of *Sw*GGAAF, we developed the first continuous assay for monitoring the enzyme activity of EAL domains. We modified a phosphate detection kit from Invitrogen by coupling it to calf intestinal phosphatase (CIP) activity. In doing this, we were able to detect the production of pGpG, which produces stoichiometric inorganic phosphate upon CIP hydrolysis, whereas c-di-GMP, the substrate of the phosphodiesterase reaction, cannot be hydrolyzed by CIP because of its cyclic structure. Table S3 of the Supporting Information summarizes data that indicate *Sw*GGAAF activity is the rate-limiting step in this novel phosphodiesterase assay. Therefore, the measured kinetics in these experiments are those of *Sw*GGAAF phosphodiesterase activity. The results of the phosphodiesterase activity assays are shown in Figure 3B, Table 2, and Table S2 of the Supporting Information.

Using this assay, a k_{cat} of 1.52 ± 0.05 s^{-1} and a K_M of 1.31 ± 0.22 μM for *Sw*GGAAF in the absence of *Sw*H-NOX were measured (Figure 3B). In general, c-di-GMP phosphodiesterases have not been kinetically characterized, perhaps because of the lack of a good continuous assay for measuring steady-state kinetics. For comparison, CC3396 from *Caulobacter crescentus*[44] is a c-di-GMP specific phosphodiesterase that is activated by GTP. The c-di-GMP turnover rate for CC3396 in the absence of GTP has been reported as 0.040 ± 0.005 s^{-1}. In the presence of 100 μM GTP, its specific activity is 1.78 ± 0.03 μM c-di-GMP (μM protein)$^{-1}$ s^{-1} and its K_M is 0.42 μM. The basal activity of *Sw*DGC (in the absence of activator) is several orders of magnitude higher than that measured for CC3396.

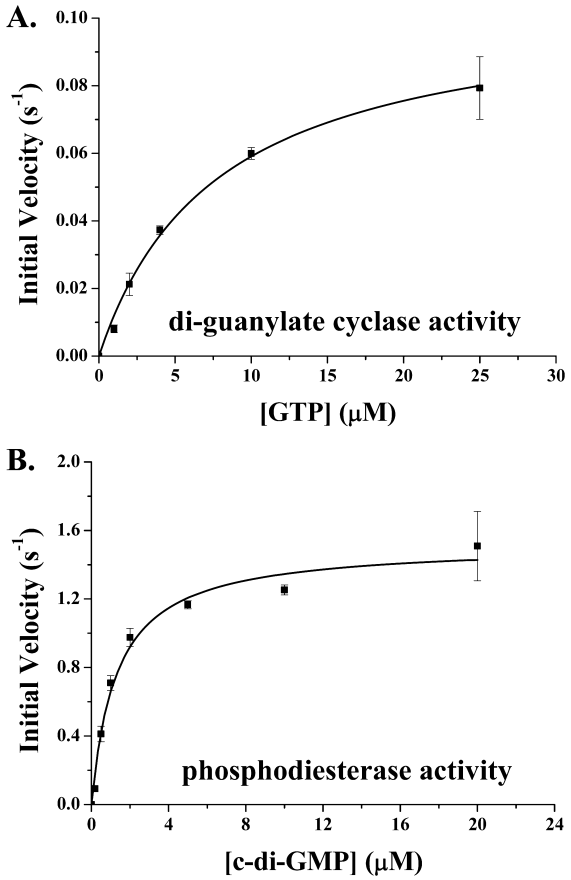

Figure 3. *Sw*DGC in the absence of *Sw*H-NOX is primarily a phosphodiesterase. (A) Steady-state kinetic analysis of the diguanylate cyclase activity of *Sw*DGC. Initial velocity of *Sw*AAL (50 nM) at 25 °C as a function of GTP concentration. (B) Steady-state kinetic analysis of the phosphodiesterase activity of *Sw*DGC. Initial velocity of *Sw*GGAAF (50 nM) at 25 °C as a function of c-di-GMP concentration. The data were fit with the Michaelis–Menten equation. Errors were determined from at least three independent trials.

In comparison to the diguanylate cyclase activity of *Sw*AAL, the k_{cat} of *Sw*GGAAF phosphodiesterase activity is 15 times higher and the K_M for c-di-GMP is 6 times lower. Therefore, as assessed by catalytic efficiency (k_{cat}/K_M), *Sw*DGC, in the absence of *Sw*H-NOX, is ~90 times more active as a c-di-GMP phosphodiesterase than a diguanylate cyclase. Therefore, we conclude that *Sw*DGC, by itself, is predominately a phosphodiesterase.

Ligand Binding Properties of *Sw*H-NOX. We hypothesize that *Sw*H-NOX is a NO sensor that regulates the enzymatic activity of *Sw*DGC. To test this hypothesis, the ligand binding properties of *Sw*H-NOX were characterized. Like all H-NOX domains, *Sw*H-NOX is a histidine-ligated protoporphyrin IX hemoprotein that senses NO through ligation to the ferrous iron atom. Thus, binding of ligand to the heme chromophore is easily monitored using electronic spectroscopy. UV–visible spectra of *Sw*H-NOX in the Fe^{2+}-unligated, Fe^{2+}–CO, and Fe^{2+}–NO complexes at room temperature are shown in Figure 4A and compared to those of sGC and other bacterial histidyl-ligated heme proteins in Table 3. Like sGC and other members of the H-NOX family from aerobic organisms, *Sw*H-NOX does not bind molecular oxygen; there is no shift in the UV–visible spectrum of the Fe^{2+}-unligated complex upon prolonged exposure to air. The ferrous complexes of *Sw*H-NOX are similar to sGC and all other H-NOX proteins characterized to date (Table 3), substantiating the membership of *Sw*H-NOX in the H-NOX family.

*Sw*H-NOX has a k_{off}(NO) of 1.5×10^{-3} s^{-1} at 20 °C (Figure S2 of the Supporting Information). This k_{off}(NO) is very similar to those of sGC and other characterized members of the H-NOX family.[22] Assuming a nearly diffusion-limited k_{on} of $\sim 4.5 \times 10^{8}$ M^{-1} s^{-1} at 20 °C, as has been observed for other H-NOX proteins,[45,46] the K_D(NO) for *Sw*H-NOX is in the picomolar range. These data indicate that *Sw*H-NOX has the properties to be a sensitive and selective NO sensor in *S. woodyi*.

Interaction of *Sw*H-NOX and *Sw*DGC. Keeping in mind our hypothesis that NO/*Sw*H-NOX regulates the activity of *Sw*DGC and having characterized *Sw*DGC and *Sw*H-NOX separately, we next investigated whether *Sw*DGC and *Sw*H-NOX interact with each other. In bacteria, co-cistronic proteins are often functional partners. A single PCR fragment from reverse transcription of *S. woodyi* mRNA confirms that *Sw*DGC and *Sw*H-NOX are in the same operon (Figure S3 of the Supporting Information).

To investigate the interaction of *Sw*H-NOX and *Sw*DGC more directly, we performed co-immunoprecipitation assays. Using GST-tagged *Sw*DGC, *Sw*AAL, *Sw*GGAAF, and GST alone as bait, His_6-tagged *Sw*H-NOX was precipitated by GST-tagged *Sw*DGC, *Sw*AAL, and *Sw*GGAAF, but not GST alone, in a pull-down assay (Figure 4B). This experiment demonstrates that *Sw*H-NOX and *Sw*DGC are binding partners. Furthermore, these data indicate that point mutations in the diguanylate cyclase and phosphodiesterase active sites do not abolish *Sw*H-NOX binding by *Sw*DGC.

NO-Bound *Sw*H-NOX Regulation of *Sw*DGC Activity. To quantify the effect of *Sw*H-NOX on *Sw*DGC activity, we determined the steady-state kinetics of both the diguanylate cyclase and phosphodiesterase activities of *Sw*DGC in the presence and absence of NO and *Sw*H-NOX. First, the effect of *Sw*H-NOX on *Sw*GGAAF phosphodiesterase activity was

Table 2. Regulation of *Sw*DGC Activity by *Sw*H-NOX[a]

enzyme	regulator	k_{cat} (s^{-1})	k_{cat}/K_M (s^{-1} μM^{-1})
*Sw*AAL (diguanylate cyclase)	without *Sw*H-NOX	0.105 ± 0.005	0.014 ± 0.002
	*Sw*H-NOX Fe^{2+}	0.209 ± 0.009	0.125 ± 0.023
	*Sw*H-NOX Fe^{2+}–NO	0.102 ± 0.011	0.011 ± 0.003
*Sw*GGAAF (phosphodiesterase)	without *Sw*H-NOX	1.52 ± 0.05	1.16 ± 0.20
	*Sw*H-NOX Fe^{2+}	1.04 ± 0.08	1.65 ± 0.59
	*Sw*H-NOX Fe^{2+}–NO	4.65 ± 0.14	15.5 ± 2.6

[a]NO-bound *Sw*H-NOX results in a decrease in c-di-GMP concentration. Kinetic parameters for diguanylate cyclase (*Sw*AAL) and phosphodiesterase (*Sw*GGAAF) activities as a function of *Sw*H-NOX in the ferrous unligated and ferrous NO-bound forms.

dx.doi.org/10.1021/bi201753f | *Biochemistry* 2012, 51, 2087–2099

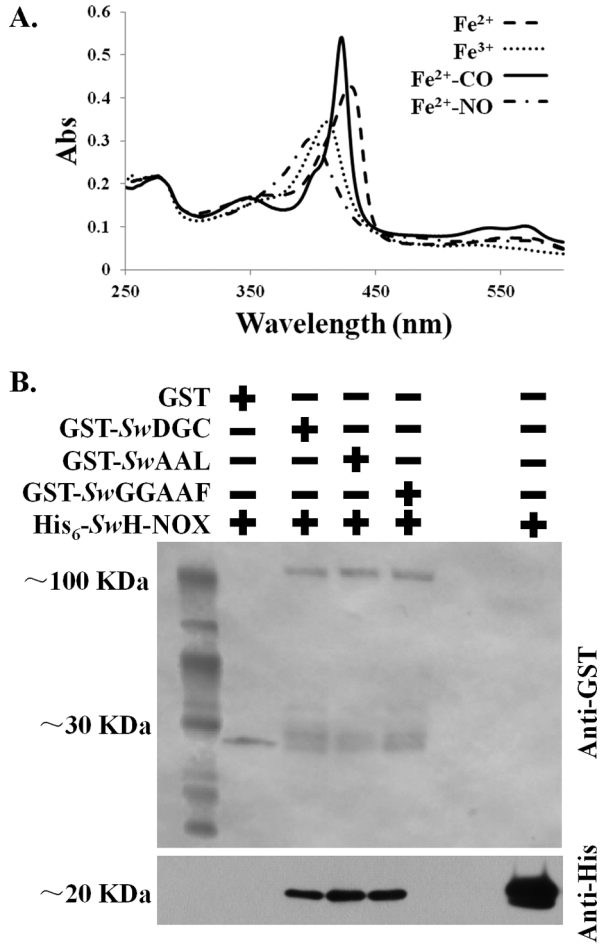

Figure 4. *Sw*H-NOX has the ligand binding properties of a NO sensor and directly binds *Sw*DGC. (A) Electronic absorption spectra of *Sw*H-NOX as the Fe^{3+}–aquo, Fe^{2+}-unligated, and Fe^{2+}–CO complexes and Fe^{2+}–NO complex at 20 °C. (B) Precipitation of *Sw*H-NOX by *Sw*DGC. GST-tagged *Sw*DGC, *Sw*GGAAF, and *Sw*AAL were used to pull down His_6-tagged *Sw*H-NOX from *E. coli* cell lysates. The top gel shows the detection of GST via an anti-GST Western blot. The far left lane contained molecular weight markers. In the next lane to the right, the bottom band is GST alone (~23 kDa, negative control). In the subsequent three lanes, the top bands are GST-*Sw*DGC, GST-*Sw*AAL, and GST-*Sw*GGAAF, respectively, and the bottom bands are GST domains proteolyzed from the larger GST-tagged constructs. The bottom gel shows detection of *Sw*H-NOX pulled down by *Sw*DGC, *Sw*AAL, and *Sw*GGAAF via an anti-His Western blot. In the far left lane, GST alone does not pull down *Sw*H-NOX (negative control). In the subsequent three lanes, *Sw*DGC, *Sw*AAL, and *Sw*GGAAF, respectively, all efficiently precipitate *Sw*H-NOX, and in the far right lane, His_6-*Sw*H-NOX (~21 kDa) was run as a positive control.

investigated. No change in the initial velocity of c-di-GMP (50 μM) turnover by *Sw*GGAAF (50 nM) was observed when varying concentrations of *Sw*H-NOX (1–20 μM) in the Fe^{2+}-unligated complex were present in the reaction mixture. However, a concentration-dependent enhancement of the initial velocity of phosphodiesterase activity was observed upon addition of NO-bound *Sw*H-NOX. In the presence of 20 μM *Sw*H-NOX in the Fe^{2+}–NO form, the initial rate of c-di-GMP hydrolysis is 1.5 times faster than in the presence of *Sw*H-NOX in the Fe^{2+}-unligated form, or in the absence of *Sw*H-NOX (Figure S4 of the Supporting Information).

Thus, we performed a full kinetic characterization of *Sw*GGAAF phosphodiesterase activity in the presence of 10 μM *Sw*H-NOX in the Fe^{2+}–NO form (Figure 5, Figure S5 of the Supporting Information, and Table 2). In the presence of

Table 3. Ligand Binding Properties of Ferrous–H-NOX Proteins from Multiple Species[a]

	Soret band (nm)				
protein	Fe^{2+}	Fe^{2+}–CO	Fe^{2+}–NO	k_{off}(NO) ($\times 10^{-4}$ s^{-1})	ref
*Sw*H-NOX	430	423	399	15.2 ± 3.5	this work
sGC[b]	431	423	398	3.6 ± 0.8	69
*Vf*H-NOX[c]	428	423	398	21 ± 0.6	29
*Vc*H-NOX[d]	429	423	398	ND[g]	70
*Lp*H-NOX[e]	428	420	398	10.3 ± 1.4	22
*So*H-NOX[f]	427	424	398	ND[g]	28

[a]Soret band electronic absorption maxima and NO dissociation rate constants are listed. [b]H-NOX from bovine lung (H-NOX is one domain of sGC). [c]H-NOX from *Vibrio fischeri*. [d]H-NOX from *Vibrio cholera*. [e]H-NOX from *L. pneumophila*. [f]H-NOX from *Shewanella oneidensis*. [g]Not determined.

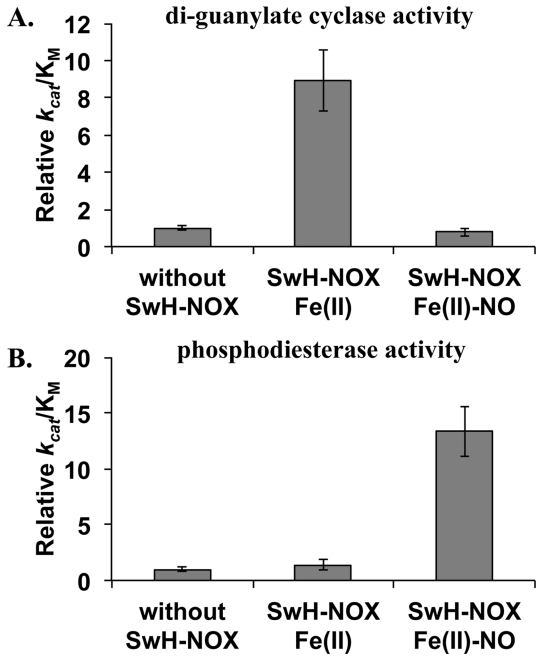

Figure 5. Upon NO binding, *Sw*H-NOX results in a decrease in c-di-GMP output by *Sw*DGC. (A) Catalytic efficiency (k_{cat}/K_M) of *Sw*DGC diguanylate cyclase activity (*Sw*AAL at 50 nM) in the presence of *Sw*H-NOX (10 μM) as the Fe^{2+}-unligated or Fe^{2+}–NO complex, relative to the catalytic efficiency of *Sw*AAL in the absence of *Sw*H-NOX. (B) Catalytic efficiency (k_{cat}/K_M) of *Sw*DGC phosphodiesterase activity (*Sw*GGAAF at 50 nM) in the presence of *Sw*H-NOX (10 μM) as the Fe^{2+}-unligated or Fe^{2+}–NO complex, relative to the catalytic efficiency of *Sw*GGAAF in the absence of *Sw*H-NOX. Errors were determined from three independent experiments.

NO-bound *Sw*H-NOX, *Sw*GGAAF has a k_{cat} of 4.65 ± 0.14 s^{-1} and a K_M of 0.30 ± 0.05 μM (Table 2). Therefore, the catalytic efficiency parameter, k_{cat}/K_M, indicates a 13-fold increase in phosphodiesterase activity when NO-bound *Sw*H-NOX is present (Figure 5B).

The effect of *Sw*H-NOX on diguanylate cyclase activity using the *Sw*AAL mutant (50 nM) was also investigated. Interestingly, a strong dose-dependent response in the initial velocity of

dx.doi.org/10.1021/bi201753f | *Biochemistry* 2012, 51, 2087–2099

diguanylate cyclase activity (50 μM GTP) as a function of Fe^{2+}-unligated *Sw*H-NOX concentration (1−10 μM) was observed, but there was no difference in the initial velocity of c-di-GMP synthesis as a function of the Fe^{2+}−NO form of *Sw*H-NOX (Figure S4 of the Supporting Information). In the presence of 10 μM *Sw*H-NOX in the Fe^{2+}-unligated form, the initial rate of c-di-GMP synthesis is 5.5 times faster than in the presence of *Sw*H-NOX in the NO-bound form or in the absence of *Sw*H-NOX. Thus, NO-bound *Sw*H-NOX has exactly the opposite effect on c-di-GMP synthesis that it has on c-di-GMP hydrolysis.

The full steady-state kinetic analysis of *Sw*AAL diguanylate activity in the presence of 10 μM *Sw*H-NOX in the Fe^{2+}-unligated form (Figure 5, Figure S5 of the Supporting Information, and Table 2) indicates that Fe^{2+}-unligated *Sw*H-NOX enhances the cyclase activity of *Sw*AAL (k_{cat} = 0.209 ± 0.009 s^{-1}; K_M = 1.67 ± 0.30 μM) by ∼10-fold in k_{cat}/K_M, as compared with *Sw*AAL diguanylate cyclase activity in the presence of NO-bound H-NOX or in the absence of H-NOX (Figure 5A and Table 2).

Therefore, unlike *Sw*DGC in the absence of *Sw*H-NOX, *Sw*H-NOX-bound *Sw*DGC acts as a diguanylate cyclase in the absence of NO. Upon exposure to NO, however, *Sw*H-NOX-regulated changes in the activities of the GGDEF and EAL domains occur. This should result in a rapid reduction in the c-di-GMP concentration. This response to NO results because NO-bound *Sw*H-NOX relieves the augmentation of diguanylate cyclase activity caused by Fe^{2+}-unligated *Sw*H-NOX and greatly activates phosphodiesterase activity

DISCUSSION

In addition to being important in many aquatic, industrial, and environmental processes, the National Institutes of Health has estimated biofilms to be responsible for up to 80% of all nonviral human microbial infections.[47,48] Despite the well-documented role of NO in the regulation of biofilm production by some bacteria, the mechanism for NO regulation of biofilm formation is unknown.[3,4,20]

We have hypothesized that the NO/H-NOX signaling pathway may be important for the development of bacterial biofilms. H-NOX domain-containing proteins are evolutionarily conserved heme proteins that include the well-characterized eukaryotic NO sensor, soluble guanylate cyclase.[45] In support of this hypothesis, H-NOX has been linked to biofilm formation,[27] and in the genomes of many bacteria, an H-NOX gene is found near a predicted DGC gene.[23] The activity of some DGC proteins is strongly correlated with biofilm growth.[49] Here evidence from genetics, biofilm growth, and enzymology experiments is presented to substantiate the link between NO/H-NOX signaling and biofilm formation.

The results of the enzyme kinetics experiments (Figures 3 and 5 and Table 2) are in excellent agreement with the biofilm growth and c-di-GMP concentration determination studies (Figures 1 and 2). On the basis of all of these data, we propose a model for NO regulation of biofilm formation in *S. woodyi* (Figure 6).

NO Causes a Reduction in the c-di-GMP Concentration through *Sw*H-NOX Regulation of the Diguanylate Cyclase and Phosphodiesterase Activities of *Sw*DGC. As illustrated in Figures 1 and 2, deletion of *Sw*H-NOX from *S. woodyi* (i.e., the Δ*hnox* strain) results in a decreased level of biofilm formation and a decreased intracellular c-di-GMP concentration. This is consistent with the

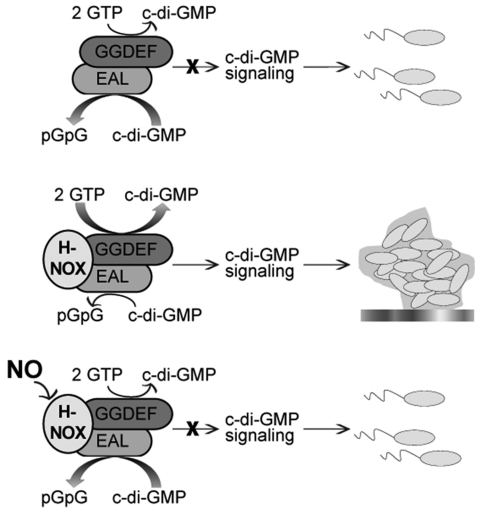

Figure 6. Our model for NO regulation of c-di-GMP synthesis in *S. woodyi*. In the absence of *Sw*H-NOX (such as in the Δ*hnox* mutant strain), *Sw*DGC is primarily a phosphodiesterase. However, it is likely that in vivo, *Sw*H-NOX and *Sw*DGC form a complex. In the absence of NO, *Sw*H-NOX is associated with *Sw*DGC and maintains its basal phosphodiesterase activity while enhancing diguanylate cyclase activity. Upon detection of NO, *Sw*H-NOX downregulates diguanylate cyclase activity and activates phosphodiesterase activity. Therefore, NO reduces the c-di-GMP concentration in *S. woodyi*, leading to a reduction in the extent of biofilm formation.

kinetic data presented in Table 2 and Figure 3, indicating that in the absence of *Sw*H-NOX, *Sw*DGC is primarily a phosphodiesterase. In this study, the mutant strain in the gene encoding *Sw*DGC was not constructed; thus, we cannot explicitly conclude that *Sw*H-NOX and *Sw*DGC form a functional complex in vivo. However, as suggested by the fact that *Sw*H-NOX and *Sw*DGC are co-cistronic (Figure S3 of the Supporting Information) and as demonstrated by our pull-down studies (Figure 4B), we propose that it is likely that *Sw*H-NOX and *Sw*DGC form a stable complex in vivo. Thus, we suggest that the *Sw*DGC kinetic data most relevant to understanding the behavior of *S. woodyi* are those for the complex with *Sw*H-NOX (Figure 5 and Table 2), as discussed below.

On the basis of the kinetic results presented in Table 2 and Figure 5, we conclude that *Sw*DGC is primarily a diguanylate cyclase in the presence of *Sw*H-NOX in the Fe^{2+}-unligated form (absence of NO). In the absence of NO, induction of recombinant *Sw*DGC and *Sw*H-NOX expression in *E. coli* results in an increase in extracellular polysaccharide matrix production (Figure S6 of the Supporting Information). This is consistent with the activity of an enzyme that is primarily producing c-di-GMP, thus acting like a diguanylate cyclase when *Sw*H-NOX, but not NO, is present. These in vitro results are supported by the biofilm growth and c-di-GMP quantification results illustrated in Figures 1 and 2, which demonstrate that wild-type *S. woodyi* (containing both *Sw*H-NOX and *Sw*DGC) has relatively high c-di-GMP concentrations and produces robust biofilms in the absence of NO.

Upon exposure to NO, wild-type *S. woodyi* experiences a decrease in c-di-GMP concentration and a decrease in biofilm thickness (Figure 2). A decrease in EPS production from *E. coli* cells expressing *Sw*DGC and *Sw*H-NOX recombinantly was observed when NO was added to the culture (Figure S6 of the Supporting Information), which is also indicative of a

downregulation in biofilm formation upon exposure to NO. These results are consistent with an increase in phosphodiesterase activity and/or a decrease in diguanylate cyclase activity, which is what is observed in steady-state kinetic assays of *Sw*DGC activity when *Sw*H-NOX and NO are present (Table 2 and Figure 5).

In our model (Figure 6), NO contributes to the regulation of biofilm formation in *S. woodyi* by simultaneously downregulating the cyclase activity and upregulating the phosphodiesterase activity of *Sw*DGC. Thus, we predict that NO could induce a rapid transition between biofilm and motility. In future experiments, we plan to test this prediction using confocal microscopy of biofilms under flow conditions. Furthermore, this model suggests that molecules that act on the NO/H-NOX pathway have the potential to be potent antibiofilm agents, a possibility that will be explored in future studies.

The mechanisms regulating biofilm dispersal are not well understood, but it is notable that NO has been shown to cause biofilm dispersal in several species.[50] Indeed, NO regulation of c-di-GMP levels has been implicated in the rapid dispersal of biofilms in *P. aeruginosa*[51] as well as other *Shewanella* species under anaerobic conditions.[52]

Biological Function of H-NOX Domains. Although there is relatively little information about the biological function of bacterial H-NOX domains to date, interestingly, it has consistently been demonstrated that NO-bound H-NOX inhibits the activity of an associated enzyme.[27,28] This is in contrast to the well-understood role of NO-bound H-NOX in upregulating the activity of mammalian sGCs.[53] Here, we demonstrate in a single H-NOX/enzyme system, that NO-bound H-NOX has both functions, that of inhibition and that of enhancement of enzymatic activity. NO-bound *Sw*H-NOX stimulates phosphodiesterase activity and inhibits diguanylate cyclase activity, in comparison to ferrous unligated *Sw*H-NOX.

This is the first time that H-NOX activation of a bacterial enzyme has been reported. It is also the first time that H-NOX regulation of more than one enzymatic activity in the same protein has been reported. In future studies, we plan to elucidate a molecular-level understanding of how *Sw*H-NOX achieves variable regulation of multiple active sites (*S. woodyi* encodes only one H-NOX). In doing so, we should be able to gain insight into how H-NOX regulates enzymatic function in general, which would enhance our understanding of both the bacterial and eukaryotic NO/H-NOX signal transduction pathways.

To understand the biological function of NO-bound H-NOX, we are also planning to investigate how the *hnox* gene is regulated. It is possible that H-NOX is constitutively expressed, to quickly respond to changing NO concentrations. On the other hand, its expression may be regulated directly by NO or some other environmental signal (related to biofilm formation or anaerobic respiration, perhaps) or by growth phase or cell density.

c-di-GMP Signaling in *Shewanella*. Although this study was primarily conducted as a model system for investigating the biological role of NO/H-NOX signaling in bacteria, there are several important implications for *Shewanella* biology suggested by our data.

Shewanella are ubiquitous in marine environments and are thought to play a role in regulating global carbon and nitrogen cycles as well as the biodegradation of marine pollutants.[54] *Shewanella* genomes generally have a very high number of GGDEF- and EAL-containing proteins; *S. oneidensis* is predicted to express 51 proteins with GGDEF domains, 27 proteins with EAL domains, and 20 proteins containing both GGDEF and EAL domains. *S. woodyi* carries genes for 45 GGDEF-containing proteins, 19 EAL-containing proteins, and 22 hybrid proteins. The large abundance of c-di-GMP synthesis and degradation proteins indicates a special role for c-di-GMP signaling in *Shewanella*, possibly because of the importance of biofilm growth for these bacteria.

Although none of the other predicted GGDEF and EAL proteins in *S. woodyi* have been characterized, our data clearly indicate that *Swoo_2751* is not the only active diguanylate cyclase in *S. woodyi* under our experimental conditions. In particular, Figure 2 indicates that c-di-GMP levels do not decrease to the baseline either in the presence of NO or in the absence of *Sw*H-NOX, each of which is a condition that downregulates diguanylate cyclase activity and upregulates phosphodiesterase activity in the *Sw*H-NOX/*Sw*DGC system reported here. It is possible that each GGDEF/EAL protein may monitor a different environmental or cellular condition and, in response to that individual stimulus (oxygen levels, carbon levels, etc.), modulate the total c-di-GMP concentration in the cell. In this model, c-di-GMP-mediated cell adhesion is an individual cell's response to the synthesis of complex information. This is consistent with other models for c-di-GMP signaling in bacteria.[55−59] It is also supportive of the "local ecological adaptation of individuals" model of biofilm formation recently suggested.[8,60−62]

Nonetheless, in this study, evidence that *Sw*DGC has a relatively large effect on overall c-di-GMP concentrations and biofilm formation (Figures 1 and 2) is presented. This large effect is underscored by the fact that *Sw*DGC is but one of 45 c-di-GMP-metabolizing enzymes predicted in the genome of *S. woodyi*. This may be because of the importance of NO as an environmental cue for *Shewanella*.

Shewanella are able to use a wide variety of molecules as alternate electron acceptors to molecular oxygen in respiration under low oxygen tension.[63] Notably, NO is an endogenous product of anaerobic respiration on nitrite and nitrate.[64,65] Thus, *S. woodyi* likely encounters NO in its environment upon reduction of nitrite when nitrate or nitrite is being used as an alternative electron acceptor. Interestingly, the interior of biofilms is thought to be anaerobic;[66] thus, generation of NO could occur in the interior of thick *S. woodyi* biofilms as a feedback signal, causing biofilm dispersal and thus preventing the biofilm community from becoming too large.

In addition to respiration on nitrate or nitrite, we have also considered other sources of NO that *S. woodyi* may encounter, including NO generated by nitric oxide synthase enzymes due to Gram-positive bacteria[67] that may be occupying the same niche as *S. woodyi*, or pathogenic or symbiotic association with eukaryotes (*S. woodyi* does not have a readily identifiable nitric oxide synthase gene in its genome). In support of a possible eukaryotic symbiotic role, *S. woodyi* is one of only a few members of the *Shewanellaceae* family that is bioluminescent, a trait that is sometimes associated with symbiosis.[68] Furthermore, *S. woodyi* was first discovered in association with squid ink.[63]

At present, the natural source of NO that causes biofilm dispersal (or a reduced level of biofilm formation) in *S. woodyi* is not known, so it is difficult for us to further speculate about the role of NO-bound H-NOX in the biology of *S. woodyi*. We note, however, that if the source of NO is anaerobic respiration on nitrate or nitrite, one might expect other *Shewanella* species

to have similar NO and biofilm responses. Interestingly, while other *Shewanella* species have H-NOXs, they are not always predicted to be in the same operon as a DGC. For example, in *S. oneidensis*, *So*H-NOX is thought to regulate phosphorylation of a histidine kinase.[28] The downstream result of this phosphorylation is not known, however, so it is possible that NO-bound H-NOX in *S. oneidensis* still feeds into c-di-GMP signaling pathways.

Regardless, we do not suppose that the NO/*Sw*H-NOX/*Sw*DGC system reported here is the only mechanism for controlling biofilm growth in *S. woodyi*. Rather, we hypothesize that NO is one of perhaps many endogenous and exogenous signals that *S. woodyi* monitors to regulate planktonic versus sessile growth.

Conclusion. The Molecular Basis of NO/H-NOX Signaling in *S. woodyi*. In this paper, we have presented data demonstrating that NO regulates biofilm formation in *S. woodyi* through changes in c-di-GMP concentration and that *Sw*H-NOX and *Sw*DGC are responsible for this NO biofilm phenotype. These results indicate that *Sw*H-NOX and *Sw*DGC directly interact and that H-NOX regulates the enzymatic activity of *Sw*DGC. In the absence of NO, *Sw*H-NOX activates the diguanylate cyclase activity of *Sw*DGC, but upon NO binding, *Sw*H-NOX downregulates cyclase activity and upregulates phosphodiesterase activity. As such, NO-bound H-NOX reduces the c-di-GMP concentration through two mechanisms, ultimately inhibiting biofilm formation.

This is among the first comprehensive studies of a diguanylate cyclase pathway, revealing how ligand binding tunes enzymatic activity to regulate intracellular c-di-GMP concentrations. Furthermore, although there have been many observations of NO regulation of biofilm formation,[3,4] this is the first demonstration of a molecular-level mechanism underlying NO regulation of c-di-GMP metabolism and biofilm formation, although such a mechanism has been suggested.[20,27]

■ ASSOCIATED CONTENT

Supporting Information

Additional steady-state kinetic controls, growth curves of wild-type and Δ*hnox* mutant *S. woodyi* as well as *E. coli* expressing recombinant *Sw*H-NOX and *Sw*DGC in the presence and absence of various concentrations of NO, NO dissociation kinetics for *Sw*H-NOX, a demonstration that *Sw*H-NOX and *Sw*DGC are in the same operon, initial velocities of *Sw*AAL and *Sw*GGAAF as a function of *Sw*H-NOX concentration, full steady-state kinetic analysis of *Sw*AAL and *Sw*GGAAF in the presence of *Sw*H-NOX as the Fe^{2+}–NO and Fe^{2+}-unligated complexes, and Congo Red staining of *E. coli* expressing recombinant *Sw*DGC and *Sw*H-NOX. This material is available free of charge via the Internet at http://pubs.acs.org.

■ AUTHOR INFORMATION

Corresponding Author

*Department of Chemistry, Stony Brook University, Stony Brook, NY 11790. Telephone: (631) 632-7945. Fax: (631) 632-7960. E-mail: elizabeth.boon@stonybrook.edu.

Funding

This work was supported by Stony Brook University and Office of Naval Research Grants N000140810738 and N000141010099 to E.M.B.

Notes

The authors declare no competing financial interest.

■ ACKNOWLEDGMENTS

We thank Roger Johnson (Stony Brook University) for helpful advice. We thank Matthew Christiansen, Coney Lin, and Ming Yang for early experiments leading to this project. We thank Sandhya Muralidharan for assistance with NO dissociation kinetic experiments.

■ ABBREVIATIONS

NO, nitric oxide; H-NOX, heme-nitric oxide/oxygen-binding; DGC, diguanylate cyclase; c-di-GMP or cyclic di-GMP, bis-(3′−5′)-cyclic dimeric guanosine monophosphate; pGpG, 5′-phosphoguanylyl-(3′−5′)-guanosine; *Sw*, *S. woodyi*; GGDEF, conserved amino acids in the catalytic site of diguanylate cyclases (the domain containing these amino acids is often termed a GGDEF domain); EAL/HD-GYP, conserved amino acids in the catalytic site of phosphodiesterases (the domain containing these amino acids is often termed an EAL/HD-GYP domain); sGC, soluble guanylate cyclase (a eukaryotic H-NOX family member); *Sw*DGC, wild-type *S. woodyi* diguanylate cyclase/phosphodiesterase protein used in this study; *Sw*GGAAF, *Sw*DGC with D287A and E288A mutations (this protein has only phosphodiesterase activity); *Sw*AAL, *Sw*DGC with the E415A mutation (this protein has only diguanylate cyclase activity); IPTG, isopropyl β-D-1-thiogalactopyranoside; CSLM, confocal scanning laser microscope; DAP, 2,3-diaminopropionic; CV, crystal violet; PVC, polyvinyl chloride; DMSO, dimethyl sulfoxide; OD, optical density; NONOate, 1-substituted diazen-1-ium-1,2-diolate nitric oxide donor that is stable as a solid but spontaneously releases NO in solution; DEA/NO, diethylamine NONOate; DETA/NO, diethylenetriamine NONOate; DPTA/NO, dipropylenetriamine NONOate; TEAA, triethylammonium acetate; HEPES, 4-(2-hydroxyethyl)-1-piperazineethanesulfonic acid; GST, glutathione *S*-transferase; Tris, tris(hydroxymethyl)aminomethane; PMSF, phenylmethanesulfonyl fluoride; DTT, dithiothreitol; CIP, calf intestinal phosphatase; CR, Congo Red; EPS, extracellular polysaccharide.

■ REFERENCES

(1) Davey, M. E., and O'Toole, G. A. (2000) Microbial biofilms: From ecology to molecular genetics. *Microbiol. Mol. Biol. Rev. 64*, 847−867.

(2) Nathan, C. (1992) Nitric oxide as a secretory product of mammalian cells. *FASEB J. 6*, 3051−3064.

(3) Schmidt, I., Steenbakkers, P., op den Camp, H., Schmidt, K., and Jetten, M. (2004) Physiologic and proteomic evidence for a role of nitric oxide in biofilm formation by *Nitrosomonas europaea* and other ammonia oxidizers. *J. Bacteriol. 186*, 2781−2788.

(4) Barraud, N., Hassett, D. J., Hwang, S.-H., Rice, S. A., Kjelleberg, S., and Webb, J. S. (2006) Involvement of Nitric Oxide in Biofilm Dispersal of *Pseudomonas aeruginosa*. *J. Bacteriol. 188*, 7344−7353.

(5) Nablo, B. J., Chen, T. Y., and Schoenfisch, M. H. (2001) Sol-gel derived nitric-oxide releasing materials that reduce bacterial adhesion. *J. Am. Chem. Soc. 123*, 9712−9713.

(6) Hetrick, E. M., Shin, J. H., Paul, H. S., and Schoenfisch, M. H. (2009) Anti-biofilm efficacy of nitric oxide-releasing silica nanoparticles. *Biomaterials 30*, 2782−2789.

(7) Privett, B. J., Nutz, S. T., and Schoenfisch, M. H. (2010) Efficacy of surface-generated nitric oxide against *Candida albicans* adhesion and biofilm formation. *Biofouling 26*, 973−983.

(8) Monds, R. D., and O'Toole, G. A. (2009) The developmental model of microbial biofilms: Ten years of a paradigm up for review. *Trends Microbiol. 17*, 73−87.

(9) Romling, U. (2011) Cyclic di-GMP, an established secondary messenger still speeding up. *Environ. Microbiol.*, DOI: 10.1111/j.1462-2920.2011.02617.x.
(10) Jenal, U. (2004) Cyclic di-guanosine-monophosphate comes of age: A novel secondary messenger involved in modulating cell surface structures in bacteria? *Curr. Opin. Microbiol. 7*, 185−191.
(11) D'Argenio, D. A., and Miller, S. I. (2004) Cyclic di-GMP as a bacterial second messenger. *Microbiology 150*, 2497−2502.
(12) Tischler, A. D., and Camilli, A. (2004) Cyclic diguanylate (c-di-GMP) regulates *Vibrio cholerae* biofilm formation. *Mol. Microbiol. 53*, 857−869.
(13) Ausmees, N., Mayer, R., Weinhouse, H., Volman, G., Amikam, D., Benziman, M., and Lindberg, M. (2001) Genetic data indicate that proteins containing the GGDEF domain possess diguanylate cyclase activity. *FEMS Microbiol. Lett. 204*, 163−167.
(14) Ryan, R. P., Fouhy, Y., Lucey, J. F., Crossman, L. C., Spiro, S., He, Y. W., Zhang, L. H., Heeb, S., Camara, M., Williams, P., and Dow, J. M. (2006) Cell-cell signaling in *Xanthomonas campestris* involves an HD-GYP domain protein that functions in cyclic di-GMP turnover. *Proc. Natl. Acad. Sci. U.S.A. 103*, 6712−6717.
(15) Simm, R., Morr, M., Kader, A., Nimtz, M., and Romling, U. (2004) GGDEF and EAL domains inversely regulate cyclic di-GMP levels and transition from sessility to motility. *Mol. Microbiol. 53*, 1123−1134.
(16) Galperin, M. Y., Nikolskaya, A. N., and Koonin, E. V. (2001) Novel domains of the prokaryotic two-component signal transduction systems. *FEMS Microbiol. Lett. 203*, 11−21.
(17) Rajagopal, S., Key, J. M., Purcell, E. B., Boerema, D. J., and Moffat, K. (2004) Purification and initial characterization of a putative blue light-regulated phosphodiesterase from *Escherichia coli*. *Photochem. Photobiol. 80*, 542−547.
(18) Karatan, E., Duncan, T. R., and Watnick, P. I. (2005) NspS, a predicted polyamine sensor, mediates activation of *Vibrio cholerae* biofilm formation by norspermidine. *J. Bacteriol. 187*, 7434−7443.
(19) Chang, A. L., Tuckerman, J. R., Gonzalez, G., Mayer, R., Weinhouse, H., Volman, G., Amikam, D., Benziman, M., and Gilles-Gonzalez, M. A. (2001) Phosphodiesterase A1, a regulator of cellulose synthesis in *Acetobacter xylinum*, is a heme-based sensor. *Biochemistry 40*, 3420−3426.
(20) Barraud, N., Schleheck, D., Klebensberger, J., Webb, J. S., Hassett, D. J., Rice, S. A., and Kjelleberg, S. (2009) Nitric oxide signaling in *Pseudomonas aeruginosa* biofilms mediates phosphodiesterase activity, decreased cyclic diguanosine-5′-monophosphate levels and enhanced dispersal. *J. Bacteriol. 191*, 7333−7342.
(21) Boon, E. M., and Marletta, M. A. (2005) Ligand discrimination in soluble guanylate cyclase and the H-NOX family of heme sensor proteins. *Curr. Opin. Chem. Biol. 9*, 441−446.
(22) Boon, E. M., Davis, J. H., Tran, R., Karow, D. S., Huang, S. H., Pan, D., Miazgowicz, M. M., Mathies, R. A., and Marletta, M. A. (2006) Nitric oxide binding to prokaryotic homologs of the soluble guanylate cyclase β1 H-NOX domain. *J. Biol. Chem. 281*, 21892−21902.
(23) Boon, E. M., Huang, S. H., and Marletta, M. A. (2005) A molecular basis for NO selectivity in soluble guanylate cyclase. *Nat. Chem. Biol. 1*, 53−59.
(24) Boon, E. M., and Marletta, M. A. (2005) Ligand specificity of H-NOX domains: from sGC to bacterial NO sensors. *J. Inorg. Biochem. 99*, 892−902.
(25) Boon, E. M., and Marletta, M. A. (2006) Sensitive and selective detection of nitric oxide using an H-NOX domain. *J. Am. Chem. Soc. 128*, 10022−10023.
(26) Iyer, L. M., Anantharaman, V., and Aravind, L. (2003) Ancient conserved domains shared by animal soluble guanylyl cyclases and bacterial signaling proteins. *BMC Genomics 4*, 5−12.
(27) Carlson, H. K., Vance, R. E., and Marletta, M. A. (2010) H-NOX regulation of c-di-GMP metabolism and biofilm formation in *Legionella pneumophila*. *Mol. Microbiol. 77*, 930−942.
(28) Price, M. S., Chao, L. Y., and Marletta, M. A. (2007) *Shewanella oneidensis* MR-1 H-NOX regulation of a histidine kinase by nitric oxide. *Biochemistry 46*, 13677−13683.
(29) Wang, Y., Dufour, Y. S., Carlson, H. K., Donohue, T. J., Marletta, M. A., and Ruby, E. G. (2010) H-NOX-mediated nitric oxide sensing modulates symbiotic colonization by *Vibrio fischeri*. *Proc. Natl. Acad. Sci. U.S.A. 107*, 8375−8380.
(30) Liu, N., Pak, T., and Boon, E. M. (2010) Characterization of a diguanylate cyclase from *Shewanella woodyi* with cyclase and phosphodiesterase activities. *Mol. BioSyst. 6*, 1561−1564.
(31) Saltikov, C. W., and Newman, D. K. (2003) Genetic identification of a respiratory arsenate reductase. *Proc. Natl. Acad. Sci. U.S.A. 100*, 10983−10988.
(32) Kovach, M. E., Elzer, P. H., Hill, D. S., Robertson, G. T., Farris, M. A., Roop, R. M. II, and Peterson, K. M. (1995) Four new derivatives of the broad-host-range cloning vector pBBR1MCS, carrying different antibiotic-resistance cassettes. *Gene 166*, 175−176.
(33) Pratt, L. A., and Kolter, R. (1998) Genetic analysis of *Escherichia coli* biofilm formation: Roles of flagella, motility, chemotaxis and type I pili. *Mol. Microbiol. 30*, 285−293.
(34) Waters, C. M., Lu, W., Rabinowitz, J. D., and Bassler, B. L. (2008) Quorum sensing controls biofilm formation in *Vibrio cholerae* through modulation of cyclic di-GMP levels and repression of vpsT. *J. Bacteriol. 190*, 2527−2536.
(35) Kharitonov, V. G., Sharma, V. S., Magde, D., and Koesling, D. (1997) Kinetics of nitric oxide dissociation from five- and six-coordinate nitrosyl hemes and heme proteins, including soluble guanylate cyclase. *Biochemistry 36*, 6814−6818.
(36) Moore, E. G., and Gibson, Q. H. (1976) Cooperativity in the dissociation of nitric oxide from hemoglobin. *J. Biol. Chem. 251*, 2788−2794.
(37) Lawrence, J. R., Korber, D. R., Hoyle, B. D., Costerton, J. W., and Caldwell, D. E. (1991) Optical sectioning of microbial biofilms. *J. Bacteriol. 173*, 6558−6567.
(38) Maragos, C. M., Wang, J. M., Hrabie, J. A., Oppenheim, J. J., and Keefer, L. K. (1993) Nitric oxide/nucleophile complexes inhibit the in vitro proliferation of A375 melanoma cells via nitric oxide release. *Cancer Res. 53*, 564−568.
(39) Keefer, L. K., Nims, R. W., Davies, K. M., and Wink, D. A. (1996) "NONOates" (1-substituted diazen-1-ium-1,2-diolates) as nitric oxide donors: Convenient nitric oxide dosage forms. *Methods Enzymol. 268*, 281−293.
(40) Pasto, M., Serrano, E., Urocoste, E., Barbacanne, M. A., Guissani, A., Didier, A., Delisle, M. B., Rami, J., and Arnal, J. F. (2001) Nasal polyp-derived superoxide anion: Dose-dependent inhibition by nitric oxide and pathophysiological implications. *Am. J. Respir. Crit. Care Med. 163*, 145−151.
(41) Pervin, S., Singh, R., and Chaudhuri, G. (2001) Nitric oxide-induced cytostasis and cell cycle arrest of a human breast cancer cell line (MDA-MB-231): Potential role of cyclin D1. *Proc. Natl. Acad. Sci. U.S.A. 98*, 3583−3588.
(42) Warwood, T. L., Ohls, R. K., Lambert, D. K., Leve, E. A., Veng-Pedersen, P., and Christensen, R. D. (2006) Urinary excretion of darbepoetin after intravenous vs subcutaneous administration to preterm neonates. *J. Perinatol. 26*, 636−639.
(43) De, N., Navarro, M. V. A. S., Raghavan, R. V., and Sondermann, H. (2009) Determinants for the Activation and Autoinhibition of the Diguanylate Cyclase Response Regulator WspR. *J. Mol. Biol. 393*, 619−633.
(44) Christen, M., Christen, B., Folcher, M., Schauerte, A., and Jenal, U. (2005) Identification and characterization of a cyclic di-GMP-specific phosphodiesterase and its allosteric control by GTP. *J. Biol. Chem. 280*, 30829−30837.
(45) Stone, J. R., and Marletta, M. A. (1996) Spectral and kinetic studies on the activation of soluble guanylate cyclase by nitric oxide. *Biochemistry 35*, 1093−1099.
(46) Zhao, Y., Brandish, P. E., Ballou, D. P., and Marletta, M. A. (1999) A molecular basis for nitric oxide sensing by soluble guanylate cyclase. *Proc. Natl. Acad. Sci. U.S.A. 96*, 14753−14758.

(47) Costerton, J. W., Cheng, K. J., Geesey, G. G., Ladd, T. I., Nickel, J. C., Dasgupta, M., and Marrie, T. J. (1987) Bacterial biofilms in nature and disease. *Annu. Rev. Microbiol. 41*, 435−464.
(48) Palmer, R. J. Jr., and Stoodley, P. (2007) Biofilms 2007: Broadened horizons and new emphases. *J. Bacteriol. 189*, 7948−7960.
(49) Garcia, B., Latasa, C., Solano, C., Garcia-del Portillo, F., Gamazo, C., and Lasa, I. (2004) Role of the GGDEF protein family in *Salmonella* cellulose biosynthesis and biofilm formation. *Mol. Microbiol. 54*, 264−277.
(50) Barraud, N., Storey, M. V., Moore, Z. P., Webb, J. S., Rice, S. A., and Kjelleberg, S. (2009) Nitric oxide-mediated dispersal in single- and multi-species biofilms of clinically and industrially relevant microorganisms. *Microb. Biotechnol. 2*, 370−378.
(51) Barraud, N., Schleheck, D., Klebensberger, J., Webb, J. S., Hassett, D. J., Rice, S. A., and Kjelleberg, S. (2009) Nitric oxide signaling in *Pseudomonas aeruginosa* biofilms mediates phosphodiesterase activity, decreased cyclic di-GMP levels, and enhanced dispersal. *J. Bacteriol. 191*, 7333−7342.
(52) Thormann, K. M., Duttler, S., Saville, R. M., Hyodo, M., Shukla, S., Hayakawa, Y., and Spormann, A. M. (2006) Control of formation and cellular detachment from *Shewanella oneidensis* MR-1 biofilms by cyclic di-GMP. *J. Bacteriol. 188*, 2681−2691.
(53) Denninger, J. W., and Marletta, M. A. (1999) Guanylate cyclase and the NO/cGMP signaling pathway. *Biochim. Biophys. Acta 1411*, 334−350.
(54) Fredrickson, J. K., Romine, M. F., Beliaev, A. S., Auchtung, J. M., Driscoll, M. E., Gardner, T. S., Nealson, K. H., Osterman, A. L., Pinchuk, G., Reed, J. L., Rodionov, D. A., Rodrigues, J. L. M., Saffarini, D. A., Serres, M. H., Spormann, A. M., Zhulin, I. B., and Tiedje, J. M. (2008) Towards environmental systems biology of *Shewanella*. *Nat. Rev. Microbiol. 6*, 592−603.
(55) Garcia, B., Latasa, C., Solano, C., Garcia-del Portillo, F., Gamazo, C., and Lasa, I. (2004) Role of the GGDEF protein family in *Salmonella* cellulose biosynthesis and biofilm formation. *Mol. Microbiol. 54*, 264−277.
(56) Kulasakara, H., Lee, V., Brencic, A., Liberati, N., Urbach, J., Miyata, S., Lee, D. G., Neely, A. N., Hyodo, M., Hayakawa, Y., Ausubel, F. M., and Lory, S. (2006) Analysis of *Pseudomonas aeruginosa* diguanylate cyclases and phosphodiesterases reveals a role for bis-(3′-5′)-cyclic-GMP in virulence. *Proc. Natl. Acad. Sci. U.S.A. 103*, 2839−2844.
(57) Lim, B., Beyhan, S., Meir, J., and Yildiz, F. H. (2006) Cyclic-diGMP signal transduction systems in *Vibrio cholerae*: Modulation of rugosity and biofilm formation. *Mol. Microbiol. 60*, 331−348.
(58) Simm, R., Lusch, A., Kader, A., Andersson, M., and Romling, U. (2007) Role of EAL-containing proteins in multicellular behavior of *Salmonella enterica* serovar *Typhimurium*. *J. Bacteriol. 189*, 3613−3623.
(59) Sommerfeldt, N., Possling, A., Becker, G., Pesavento, C., Tschowri, N., and Hengge, R. (2009) Gene expression patterns and differential input into curli fimbriae regulation of all GGDEF/EAL domain proteins in *Escherichia coli*. *Microbiology 155*, 1318−1331.
(60) Klausen, M., Heydorn, A., Ragas, P., Lambertsen, L., Aaes-Jorgensen, A., Molin, S., and Tolker-Nielsen, T. (2003) Biofilm formation by *Pseudomonas aeruginosa* wild type, flagella and type IV pili mutants. *Mol. Microbiol. 48*, 1511−1524.
(61) Klausen, M., Gjermansen, M., Kreft, J. U., and Tolker-Nielsen, T. (2006) Dynamics of development and dispersal in sessile microbial communities: Examples from *Pseudomonas aeruginosa* and *Pseudomonas putida* model biofilms. *FEMS Microbiol. Lett. 261*, 1−11.
(62) Ghigo, J. M. (2003) Are there biofilm-specific physiological pathways beyond a reasonable doubt? *Res. Microbiol. 154*, 1−8.
(63) Makemson, J. C., Fulayfil, N. R., Landry, W., Van Ert, L. M., Wimpee, C. F., Widder, E. A., and Case, J. F. (1997) *Shewanella woodyi* sp. nov., an exclusively respiratory luminous bacterium isolated from the Alboran Sea. *Int. J. Syst. Bacteriol. 47*, 1034−1039.
(64) Zumft, W. G. (2002) Nitric oxide signaling and NO dependent transcriptional control in bacterial denitrification by members of the FNR-CRP regulator family. *J. Mol. Microbiol. Biotechnol. 4*, 277−286.
(65) Ji, X. B., and Hollocher, T. C. (1988) Reduction of nitrite to nitric oxide by enteric bacteria. *Biochem. Biophys. Res. Commun. 157*, 106−108.
(66) Stewart, P. S., and Franklin, M. J. (2008) Physiological heterogeneity in biofilms. *Nat. Rev. Microbiol. 6*, 199−210.
(67) Schreiber, F., Beutler, M., Enning, D., Lamprecht-Grandio, M., Zafra, O., Gonzalez-Pastor, J., and de Beer, D. (2011) The role of nitric-oxide-synthase-derived nitric oxide in multicellular traits of *Bacillus subtilis* 3610: Biofilm formation, swarming, and dispersal. *BMC Microbiol. 11*, 111.
(68) Widder, E. A. (2010) Bioluminescence in the Ocean: Origins of Biological, Chemical, and Ecological Diversity. *Science 328*, 704−708.
(69) Stone, J. R., and Marletta, M. A. (1994) Soluble guanylate cyclase from bovine lung: Activation with nitric oxide and carbon monoxide and spectral characterization of the ferrous and ferric states. *Biochemistry 33*, 5636−5640.
(70) Karow, D. S., Pan, D., Tran, R., Pellicena, P., Presley, A., Mathies, R. A., and Marletta, M. A. (2004) Spectroscopic characterization of the soluble guanylate cyclase-like heme domains from *Vibrio cholerae* and *Thermoanaerobacter tengcongensis*. *Biochemistry 43*, 10203−10211.